Improvement of electrochemical properties of $LiNi_{1/3}Co_{1/3}Mn_{1/3}O_2$ by coating with V_2O_5 layer

Xizheng Liu[1,2], Ping He[1], Huiqiao Li[1], Masayoshi Ishida[2], Haoshen Zhou[1*]

1. Energy Technology Research Institute, National Institute of Advanced Industrial Science and Technology (AIST), Umezono 1-1-1, Tsukuba, 305-8568, Japan.
2. Graduate School of System and Information Engineering, University of Tsukuba, Tennoudai 1-1-1, Tsukuba, 305-8573, Japan.

[*] Corresponding author. Tel.:81-29-861-5782; Fax:81-29-861-3489.

E-mail: hs.zhou@aist.go.jp (Haoshen Zhou)

Headings

V_2O_5 has been coated on layered $LiNi_{1/3}Co_{1/3}Mn_{1/3}O_2$. Its rate and cycle capacities have been improved by surface coating. CV and EIS on before and after cycled cells have been conducted to illustrate the effect of the V_2O_5 coating layer.

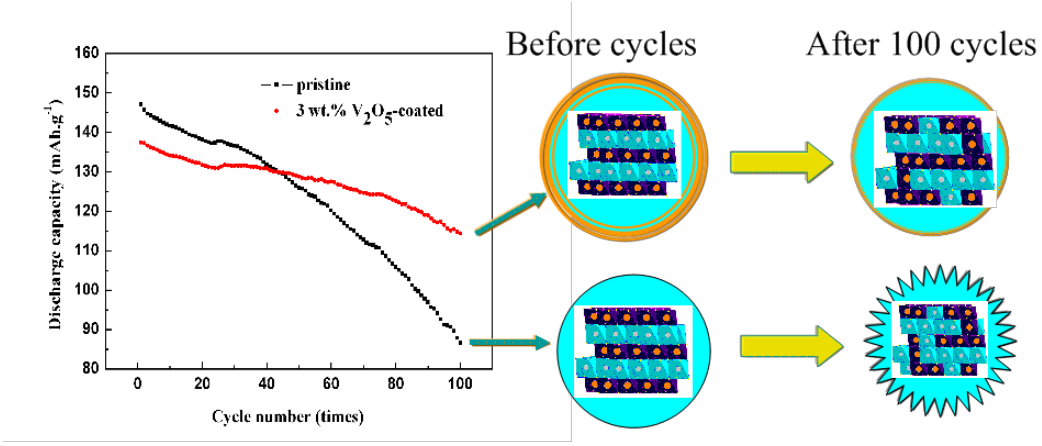

Abstract

The capacity fading and lower rate of layered cathode materials prohibited widely applications in lithium ion batteries. In this paper, V_2O_5 was coated on the surface of $LiNi_{1/3}Co_{1/3}Mn_{1/3}O_2$ to enhance its electrochemical performance at a voltage range of 2.8-4.5 V. The prepared materials were characterized by powder X-ray diffraction (XRD), Scanning electron microscopy (SEM) and Transmission electron microscope (TEM). The capacity retention at the 100^{th} cycle have been increased from 62% to over 80% for the 3 wt% V_2O_5 coated sample.The rate performance have been improved by V_2O_5 coating which mainly because of the coating layer enhance the surface electronic/ionic transport. Cyclic Voltammetry (CV) showed that the redox properties of the pristine sample have a more obvirous changes after charge-discharge cycles compared with the coated samples. Electrochemical impedance spectroscopy (EIS) results suggest that the V_2O_5 coating layer play an important role in suppressing the increase of cell impedance with cycling especially for the increase of charge-transfer resistance (R_{ct}).

Keyword $LiNi_{1/3}Co_{1/3}Mn_{1/3}O_2$ · Surface modification · V_2O_5 coating · Cycling performance · Charge-transfer resistance

1. Introduction

Lithium ion batteries (LIB) have been intensively studied due to their desirable properties as high power and energy densities, good cycle performance and long calendar life. There are great demands for their use as power sources for various electronic equipments such as laptop computers, cordless telephones, storing wind and solar energy in smart grids and other portable consumer electronic devices [1-3]. At present, the cathode materials for LIB in portable electronic products are mainly $LiCoO_2$ due to its ease production and well electrochemical properties [4-6]. However, the scarcity source and toxicity of $LiCoO_2$ have prompted scientists to look for other alternative cathode materials in view of economy and safety. $Li[Ni_{1/3}Co_{1/3}Mn_{1/3}]O_2$ is one of the most competitive candidate to replace the commercial $LiCoO_2$ because of its high capacity, safety and low cost [7-8]. However, there is a obviously capacity fading of $Li[Ni_{1/3}Co_{1/3}Mn_{1/3}]O_2$ at high cycling rate which prohibited widely application of this materials [9-10]. The most plausible reasons are the lower ionic/electronic conductivity and side reactions at the interface of the electrode and electrolyte [11].

Recently, surface modification have been proved to be a facile and effective strategy to improve the electrochemical performance of cathode materials [12-14]. When an inactive material, which can not react with the electrolyte, was coated on the surface of cathode materials, it can suppress the side-reaction between the electrolyte and electrode [15-17]. It can also provide electron-conducting media that facilitates the charge transfer at the surface of particles [6]. Up to now, various metals (e.g., Ag) [18], metal oxides (e.g., Al_2O_3, ZrO_2, CeO_2) [19-21], metal fluorides(e.g., ZrF_2, AlF_3, SrF_2) [22-24], $LiAlO_2$ [25] and some carbon composites (e.g., PPy, graphene) [26-27] have been coated on the surface of $Li[Ni_{1/3}Co_{1/3}Mn_{1/3}]O_2$. Recent research progresses prove that amorphous vanadium oxide have became one of the most attractive candidates as coating material for it acts as an ion and electrons double conductive materials [28]. K. S. Park et al. reported that VO_x impregnated $LiFePO_4$ with improved rate capacities [28]. They also reported that VO_x impregnated $0.5Li_2MnO_3$-$0.5LiNi_{0.4}Co_{0.2}Mn_{0.4}O_2$ cathode materials showed an improved electrochemical performance for the vanadium ions in $3d^0$ electronic states during high voltage charging state could reduce the surface catalytic activities and stabilize the surface oxide ions during their electrochemical oxidation [29]. J. W. Lee et al. reported that a vanadium

oxide coating layer on $LiCoO_2$ improved the cycleability at a high-charge cut-off voltage [30]. A suppression of dissolution of Mn from spinel $LiMn_2O_4$ by coating with VO_x layer have also been reported by J.Cho [31]. However, the effects of the VO_x coating layer on $Li[Ni_{1/3}Co_{1/3}Mn_{1/3}]O_2$ have still not been investigated.

In the present study, we have explored the possibility of coating the $LiNi_{1/3}Co_{1/3}Mn_{1/3}O_2$ particles by a V_2O_5 layer. We adopted the sol-gel method to get a uniform V_2O_5 coating layer. The effect of the V_2O_5 coating layer on the structure and morphology have also been studied. The charge-discharge properties at a high rate and also the rate performance have been explored. Cyclic voltammetry (CV) and electrochemical impedance spectroscopy (EIS) on cycled cells with different times were used to investigate the mechanism of the improvement in the electrochemical properties of the V2O5 coated $LiNi_{1/3}Co_{1/3}Mn_{1/3}O_2$ material.

2. Experiment

Pristine $LiNi_{1/3}Co_{1/3}Mn_{1/3}O_2$ powder was synthesized by carbonate precipitation method according the reference [32]. The coating process was conducted by sol-gel method. The V_2O_5 hydrosol was first obtained by adding of certain amount of V_2O_5 and H_2O_2 to 5 ml deionized water with vigorously stiring. And then $LiNi_{1/3}Co_{1/3}Mn_{1/3}O_2$ (1 g) was added to the hydrosol, kept on stiring for 2 h at room temperature. After Ultrasonic treatment for 10 minutes, the suspension was dried at 80 °C. The final powder was heat-treated in a furnace at 350 °C for 5 h in air. For comparing, the pristine samples had also been heat-treated under the same conditions.

The structure of the powder samples of pristine and coated samples were analyzed using a Bruker D8 Advance X-Ray powder Diffractometer (XRD) with Cu *K*α radiation. The morphology of all the samples were examined using Scanning Electronic Microscope (SEM) on a JSM-6700F instrument and Transmission electron microscope (TEM) on a JEOL 3100F with a voltage of 300 KV.

The electrochemical performance of the pristine and V_2O_5 coated $Li[Ni_{1/3}Co_{1/3}Mn_{1/3}]O_2$ cathodes were conducted by coin cells (CR 2032) consisting of a cathode, metallic lithium anode, polypropylene separator, and an electrolyte of 1M $LiPF_6$ in EC/DEC (1:1 vol%). The cathode contained 80 wt% active materials, 15 wt% acetylene black, and 5 wt% polytetrafluoroethylene (PTFE) binder. The above mixture were mixed and ground in a agate mortar and then pressed onto

a aluminum mesh which served as a current collector and dried at 80 °C for 12 h under vacuum. The cells were assembled in an Ar-filled glove box and subjected to galvanostatic cycling using a Hokuto Denko in a potential range of 2.8-4.5 V (versus Li^+/Li) at currents of 150 mAh/g and 300 mAh/g. The specific capacity and current density are base on the synthesized cathode materials, for the coated materials, the coating layer have been included. The Cyclic Voltammetry (CV) were done with coin cells on a Solartron Instrument Model 1287 in the voltage range of 2.8-4.5 V (versus Li^+/Li) with a scan rate of 0.2 mV/s. The electrochemical impedance spectroscopy (EIS) were also done with coin cells on a Solartron Instrument Model 1287 electrochemical interface and a 1255 B frequency response analyzer controlled by Z-plot. The measurements were performed in the frequency range 0.5 MHz to 0.05 Hz with an AC signal amplitude of 5 mV. Data analysis used the software Zview 2.70. (Scribner Associates Inc., USA)

3. Result and discussion

XRD patterns of the pristine $LiNi_{1/3}Co_{1/3}Mn_{1/3}O_2$ and 3 wt%-V_2O_5-coated $LiNi_{1/3}Co_{1/3}Mn_{1/3}O_2$ are presented in Fig. 1a. The patterns showed that the synthesized materials have highly crystalline and all the diffraction peaks could be indexed as a layered oxide structure which based on a hexagonal α-$NaFeO_2$ structure with a space group of *R*-3m. The splitting of the peaks (108), (110) and (006), (102) in the XRD patterns indicated that the materials had a well ordered α-$NaFeO_2$ structure, $I_{003}/I_{104}>1.2$ was an indication of desirable cation mixing [33]. The lattice parameters of pristine and V_2O_5 coated sample were summarized in Table 1. It is clear that there is no significant difference before and after surface coating by V_2O_5. The relatively low heat treatment temperature of the V_2O_5 coating layer seemed not allow for the formation of a solid solution between the V_2O_5 coating layer and the pristine $LiNi_{1/3}Co_{1/3}Mn_{1/3}O_2$ materials. It demonstrated that the layered structure of $LiNi_{1/3}Co_{1/3}Mn_{1/3}O_2$ had not been affected by coating. No impurities or secondary phases was observed in this figure. In order to confirm the contents of coating layer, we also synthesized the V_2O_5 powder using the same synthesis route without adding of layered material $LiNi_{1/3}Co_{1/3}Mn_{1/3}O_2$. The XRD patterns (in Fig. 1b) showed that it can be indexed as compound V_2O_5 with space group of P_{mmn} and the JCPDS card 41-1462. So the coating layer can be considered as V_2O_5.

The surface morphologies of the pristine and 3 wt%-V_2O_5-coated samples were observed by

SEM and TEM. As shown in Fig. 2a and 2c, the secondary particles of pristine $LiNi_{1/3}Co_{1/3}Mn_{1/3}O_2$ (from 2 μm to several μm) consisted of primary particles (300-500 nm in size). We can see clearly that the surface and edge of the particles are smooth and clean from TEM image in Fig. 2e. In contrast, after coating with V_2O_5, the particle is almost no changes in size(Fig. 2b and 2d), but the surface became considerably rough and ambiguous (as shown in Fig.2f), the coating layer is about 5-8 nm. These figures revealed that the V_2O_5 was successfully coating on the pristine $LiNi_{1/3}Co_{1/3}Mn_{1/3}O_2$.

The SEM-energy dispersive spectrometry (EDS) measurement have been conducted to get the directly evidence of the composition and distribution of vanadium in 3 wt% V_2O_5-coated $LiNi_{1/3}Co_{1/3}Mn_{1/3}O_2$ as shown in Fig.3a-3c. Based on the mapping, V in the sample is homogeneously distributed in the composite, indicating uniform distribution of vanadium oxide on the surface of $LiNi_{1/3}Co_{1/3}Mn_{1/3}O_2$. X-ray photoelectron spectroscopy (XPS) were employed to reveal subtle information of the surface structure. Fig.3d shows that the binding energies of electrons in V 2p3 are located at 516.9 and 515.8 eV. These two peaks related to the formal oxidation degrees of +5 and +4, corresponding to the vanadium oxides V_2O_5 and VO_2, respectively.[29] The peak intensity for V^{4+} is less than 10% compared with the peak intensity for V^{5+}. Therefore, the major component in the coating layer is V_2O_5.

The capacity, cyclic performance and rate capability of pristine and coated $Li[Ni_{1/3}Co_{1/3}Mn_{1/3}]O_2$ electrode were characterized to investigate the coating effect. The cycle performance of the pristine and coated samples with different V_2O_5 coating contents are shown in Fig. 4a. The charge-discharge were conducted between 2.8-4.5 V at a current of 150 mA/g. With 1 wt%, 2 wt%, 3 wt%, 4 wt% and 5 wt% V_2O_5 coating, the discharge capacities are 111.5, 118.7, 140.1, 128.0 and 124.8 mAh/g at the 100^{th} cycle, respectively. Meanwhile, the discharge capacity is 103.2 mAh/g for the pristine $Li[Ni_{1/3}Co_{1/3}Mn_{1/3}]O_2$ at the 100^{th} cycle. It is clearly indicated that the cycle performance have been improved by V_2O_5 coating. The optimal coating amount is 3 wt% according the capacity retention.

The cycle performance at a relatively high charge-discharge current of 300 mA/g was also examined on pristine and 3 wt% V_2O_5-coated $Li[Ni_{1/3}Co_{1/3}Mn_{1/3}]O_2$ as shown in Fig. 4b. The pristine sample showed a higher initial discharge capacity than the coated samples, but it suffered a serious capacity fading upon cycling. In contrast, the coated samples showed a relatively smaller

initial discharge capacity, there is a slight capacity fading upon cycling. Table 2 summarized the discharge capacity for the 1st, 50th and 100th cycles of the pristine and coated electrodes. At the 50th cycle, the two samples showed similar discharge capacities of 126 mAh/g (pristine samples) and 129 mAh/g (3 wt% V_2O_5-coated samples). But at the 100th cycle, the pristine only showed a discharge capacity of 87 mAh/g and retained 59.2% of its original capacity of approximately. However, the 3 wt% V_2O_5-coated materials showed higher capacities of 114 mAh/g and displayed 83.2% retention of the initial discharge capacity. It can be clearly concluded that the capacity fading has been suppressed by surface coating of V_2O_5. The most possible reason for the capacity fading is side-reaction between electrode and electrolyte during extensive cycling. For the coated samples, the V_2O_5 coating layer acted as a protective layer, it prevented the directly contact between the active electrode material and electrolyte, therefore, it impeded the side reactions in this aera upon charge-discharge cycles.

Fig.5a shows the first charge/discharge profiles of the pristine and 3 wt% V_2O_5 coated materials between 2.8-4.5 V at a current of 300 mA/g. The charge-discharge curves showed typical potential plateaus of layered compounds at 3.9 V region, which originating from the Ni^{2+}/Ni^{4+} redox couples [34]. The pristine $Li[Ni_{1/3}Co_{1/3}Mn_{1/3}]O_2$ presented a charge capacity of 180.9 mAh/g and discharge capacity of 147 mAh/g at the first cycle, however, there were a little lower charge-discharge capacities for coated samples. For the 3 wt% V_2O_5-coated sample, the charge capacity was 168.3 mAh/g and discharge capacity was 137 mAh/g at the first cycle. The reason for lower initial capacities of the coated materials is that the V_2O_5 coating layer showed no capacity contribution at the voltage above 2.8 V. It can also be explained by the V^{5+}/V^{4+} redox not occurred in the experiment condition according cyclic voltammetry measurements as shown in the following results. Fig. 5b presents the discharge capacity retentions of the pristine and coated samples at different rates in a range of 2.8-4.5 V. The coated samples clearly shows a better discharge capacity than the pristine when the rate is larger than 450 mA/g. This result indicates that a V_2O_5 coating layer assist the lithium ions and electrons transport at the electrode surface. This effects are more obvious at high rates. The capacity recovery of the coated sample, when took the charge-discharge at 75 mA/g rate again after high rate cycling, were better (93.6% for 3 wt% V_2O_5 coated sample) than the pristine samples (90%). This result also confirm that the coating layer can impede the capacity fading.

In order to detailed study the changes of charge-discharge processes with cycles, Fig. 6 shows the charge and discharge curves of pristine and V_2O_5-coated materials at different cycles. During the charge processes, the plateaus of the two samples appeared at about 3.8 V and slowly increased to 4.5 V. For the pristine sample, the plateaus became higher as cycling and reached to about 4.05 V at the 100^{th} cycle. But for the coated samples, the changes was smaller and the plateaus were 3.91 V at the 100^{th} cycle. For the discharge processes of the pristine sample, the plateaus became more and more vague with cycling. In contrast, the changes of the plateau for the coated samples were minor. The increase of the separations between charge plateau and discharge plateau originated from the increase of overpotential which caused by the side-reactions between the electrode and electrolyte. The V_2O_5 coating layer suppressed side-reactions at the interface of electrode/electrolyte and so the coated samples showed smaller changes of the charge-discharge plateaus than the pristine sample.

Cyclic voltammetry (CV) is an effective analysis technique for studying the oxidation/reduction processes in electrode reaction. It should be pointed out that the redox potentials of ions do depend on the metal-metal interactions within the layers [35]. Therefore, for layered cathode materials, the changes of the metal circumstance which caused by the increase of cation mixing can be reflected by cyclic voltamgrams. In our research, CV were conducted to investigate the oxidation/reduction properties on before and after cycled cells. As shown in Fig.7a, the pristine sample showed a well refined redox peaks at 3.887 and 3.689V, while the coated samples showed peaks at 3.866 V and 3.697V, which can be assigned to the Ni^{2+}/Ni^{4+} couple [33]. It suggests that the coated V_2O_5 layers do not take participate in the redox reaction in the voltage range of 2.8-4.5 V. It should also be noted that the separation of cathodic and anodic peaks of coated sample is smaller than that of the pristine samples, which suggested that the polarization of the electrode was decreased due to the improved surface conductivity by surface coating. To further understanding the changes of redox properties of the materials, the CV response of the cells cycled 100 times have also been conducted as shown in Fig. 7b. The cathodic peaks of the 3 wt% V_2O_5 coated samples shifted to a higher voltage side by 0.1 V and the anodic peaks get shifted to a lower voltage side by 0.05-0.07 V. The shift of the peaks originated from either the side reactions between the electrodes and electrolytes or polarization on the surface of the electrodes. The pristine samples, however, underwent a more manifest changes during the redox processes. The cathodic peak shifted to

4.117 V while the anodic peaks became indistinct. This means that the pristine electrode underwent an intense surface and structure changes by side reactions during charge-discharge cycles. This behavior implies that the V_2O_5 surface layer relieved the side-reactions between the electrode and electrolyte on cycling by preventing directly interactions between electrode and electrolyte.

In order to further study how the coating layer suppressing the side-reactions between the electrode and electrolyte, the electrochemical impedance spectroscopy (EIS) measurements were carried out after the 2nd and 100th charge-discharge cycles. For each measurement, the cells were first galvanostatically cycled to the desired cycle numbers (between 4.5 V and 2.8 V at the current of 300 mA/g), followed by charging them to 4.5 V at a small current of 15 mA/g, discharged to 3.8 V at the same current, and then allowed the cell to relax to its open circuit potential for 3 h. Fig. 8a and Fig. 8b show the Nyquist plots of both of the samples. The impedance spectra were fitted by the equivalent circuit model as shown in Fig. 8c. The R_{sol} represents electrolyte resistance, R_{sei} represents the impedance of the natural and artificial solid electrolyte interface and the impedance of electrons through the active materials. This part corresponds to the first semicircle from the high to medium frequency region in the Nyquist plots. The R_{ct} represents the charge transfer resistance which corresponding to the second semicircles in the low-frequency region. And the last parts in the lowest frequency region are due to the diffusion of lithium ions in the solid electrodes, as introduced by Warburg [21]. The fitting results are depicted in Table 3. At the second cycle, the R_{sei} value of the 3 wt% V_2O_5-coated material is 27.55 Ω, however, for the pristine samples, the R_{sei} value is only 6.92 Ω. Because at the initial state of the battery, the amorphous V_2O_5 layer produced a resistance for the transfer of Li^+ ions and electrons in the electrode and electrolyte interface layer. Upon cycling, the R_{sei} value of pristine samples increased rapidly. The side reactions made the surface of electrodes become rough, and the transfer of charge and electrons at this region became more and more difficult. Both of the two samples showed small charge transfer resistance at the second cycles. So it (R_{ct}) played a minor role at the initial stage of the cycles. But the R_{ct} values of the pristine electrode increased faster than the V_2O_5-coated materials upon cycling. The R_{ct} value of the pristine material was 12.04 Ω at the second cycle, rapidly increased to 267.1 Ω at the 100th cycles. However, for 3 wt% V_2O_5-coated sample, the R_{ct} values was 16.31 Ω at the second cycle and slowly increased to 141.6 Ω at the 100th cycle. The abrupt increase in charge-transfer

resistance of the $Li[Ni_{1/3}Co_{1/3}Mn_{1/3}]O_2$ has been reported by others, and considered as the main reasons for the capacity fading [9]. From the EIS data, we can conclude that the V_2O_5-coating layer can stable the interface of electrode/electrolyte and slow down the increase of charge transfer resistance. And also it in turns limits the increase of the total cell resistance and suppress the capacity fading of the V_2O_5-coat $Li[Ni_{1/3}Co_{1/3}Mn_{1/3}]O_2$.

4. Conclusion

V_2O_5 has been uniformly coated on the surface of layered $Li[Ni_{1/3}Co_{1/3}Mn_{1/3}]O_2$, and its effects on electrochemical properties have also been investigated. The one with 3 wt% V_2O_5-coated sample showed the best performance in terms of cycle and rate capacities. After 100 cycles, discharge capacities retention have been improved from 59.2% to 83.2% by V_2O_5-coating. As evidenced by CV and EIS, the V_2O_5-coating layer suppressed the side-reactions between the electrode and electrolyte and the increase of charge-transfer resistance upon cycling. This study demonstrated that surface coating with V_2O_5 can be used to enhance the high rate electrochemical properties of the layered cathode materials for lithium ion battery.

Acknowledgements: X. Z. Liu would like to thank Dr. Tianyou Zhai in NIMS Japan, Dr. Nokuko Hanada and Prof. Waichi Iwasaki in University of Tsukuba for valuable discussions and suggestions.

References

[1] J. B. Goodenough, Y. Kim, Chem. Mater. 22 (2010) 587-603.

[2] J. H. Ju, K. A. Ryu, J. Alloy Compd. 509 (2011) 7985-7992.

[3] R. Marom, S. F. Amalraj, N. Leifer, D. Jacob, D. Aurbach, J. Mater. Chem. 21 (2011) 9938-9954.

[4] J. Gainese, R. Cuenza, in: Report ANL/ESD-42, Argonne National Laboratory, Argonne, IL, 2000.

[5] J. Li, C.Daniel, D.Wood, J. Power Source 196 (2011) 2452-2460.

[6] Z. Chen, Y. Qin, K. Amine, Y. K. Sun, J. Mater. Chem. 20 (2010) 7606-7612.

[7] T. Ohzuku, Y. Makimura, Chem. Letter 30 (2001) 642-643.

[8] R. Guo, P. F. Shi, X. Q. Cheng, C. Y. Du, J. Alloy Compd. 473 (2009) 53-59.

[9] J. Li, L. Wang, Q. Zhang, X. He, J. Power Source 190 (2009) 149-153.

[10] K. C. Jiang, S. Xin, J. S. Lee, J. Kim, X. L. Xiao, Y. G. Guo, Phys. Chem. Chem. Phys. 14 (2012) 2934-2939.

[11] H. Miyashiro, A. Yamanaka, M. Tabuchi, A. Seki, M. Bakayama, Y. Ohno, Y. Kobayashi, Y. Mita, A. Usami, M. Wakihara, J. Electrochem. Soceity 153 (2006) A348-A353.

[12] H. Q. Li, H. S. Zhou, Chem. Commun. 48 (2012) 1201-1217.

[13] X. Z. Liu, H. Q. Li, E. Yoo, M. Ishida, H. S. Zhou, Electrochim. Acta 83 (2012) 253-258.

[14] S. T. Myung, K.Amine, Y. K. Sun, J. Mater. Chem. 20 (2011) 7074-7095.

[15] Y. K. Sun, S. W. Cho, S. T. Myung, K. Amine, J. Prakash, Electrochim. Acta 53 (2007) 1013-1019.

[16] Z. Chen, J. R. Dahn, Electrochim. Acta 49 (2004) 1079-1090.

[17] Z. Chen, J. R. Dahn, Electrochem. Solid State Letter 6 (2003) A221-A224.

[18] R. Guo, P. Shi, X. Cheng, Y. Ma, Z. Fan, J. Power Source 189 (2009)2-8.

[19] S. K. Hu, G. H. Cheng, M. Y. Cheng, B. J.Hwang, R. Santhanam, J. Power Source 188 (2009) 564-589.

[20] M. Wang, F. Wu, Y. F. Su, S. Chen, Science China Series E 52 (2009) 2737-2741.

[21] L. A. Riley, A. V. Atta, A. S. Cavanagh, Y. Yan, S. M. George, P. Liu, A. C. Dillon, S. H. Lee, J. Power Source 196 (2011) 3317-3324.

[22] S. H. Yun, K. S. Park, Y. J. Park, J. Power Source 195 (2010) 6108-6115.

[23] K. S. Lee, S. T. Myung, D. W. Kim, Y. K. Sun, J. Power Source 196 (2011) 6974-6977.

[24] Y. K. Sun, S. W. Cho, S. W. Lee, C. S. Yoon, K. Amine, J. Electrochem. Soceity 154 (2007) A168-A172.

[25] H. S. Kim, Y. Kim, S. Kim, S. W. Martin, J. Power Source 161 (2006) 623-627.

[26] P. Zhang, L. Zhang, X. Ren, Q. Yuan, J. Liu, Q. Zhang, Synthetic Metal 161 (2011) 1092-1097.

[27] C. V. Rao, A. L. M Raddy, Y. Ishikawa, P. M. Ajayan, ACS Applied Mater Interface 3 (2011) 2966-2972.

[28] K. S. Park, A. Benayad, M. S. Park, A. Yamada, S. G. Doo, Chem. Commun. 46 (2010) 2572-2574.

[29] K. S. Park, A. Benayad, M. S. Park, W. Choi, D. Im, Chem. Commun. 46 (2010) 4190-4192.

[30] J.W. Lee, S. M. Park, H. J. Kim, J. Power Source 188 (2009) 583-587.

[31] J.Cho, J. Mater. Chem. 18 (2008) 2257-2261.

[32] J. Wang, X. Yao, X. Zhou, Z. Liu, J. Mater. Chem. 21 (2011) 2544-2549.

[33] K. M. Shaju, G. V. Subba, B. V. R. Chowdari, Electrochim. Acta 48 (2002) 145-151.

[34] Y. Koyama, N. Yabuuchi, I. Tanaka, H. Adachi, T. Ohzuku, J. Electrochem. Soceity 154 (2004) A1545-A1551.

[35] J. Reed, G. Ceder, Electrochem. Solid State Letter 5 (2002) A145-A148.

Table 1 Lattice parameters of Pristine $LiNi_{1/3}Co_{1/3}Mn_{1/3}O_2$ and 3% V_2O_5-coated $LiNi_{1/3}Co_{1/3}Mn_{1/3}O_2$

Sample	a (Å)	c (Å)	V ($Å^3$)
Pristine $LiNi_{1/3}Co_{1/3}Mn_{1/3}O_2$	2.8608(6)	14.2334(50)	100.88(5)
3 wt% V_2O_5-coated $LiNi_{1/3}Co_{1/3}Mn_{1/3}O_2$	2.8584(8)	14.2295(69)	100.68(8)

Table2 Discharge capacities of pristine and V_2O_5-coated $LiNi_{1/3}Co_{1/3}Mn_{1/3}O_2$ electrodes during 100 cycles in the voltage range of 4.5-2.8 V

	1^{st} (mAh/g)	50^{th} (mAh/g)	100^{th} (mAh/g)
Pristine	147	126	87
3 wt% V_2O_5-coated	137	129	114

Table 3 Fitting results of the AC impedance parameters

Samples	R_{sol} (Ω) At the 2^{nd}	R_{sol} (Ω) At the 100^{th}	R_{sei} (Ω) At the 2^{nd}	R_{sei} (Ω) At the 100^{th}	R_{ct} (Ω) At the 2^{nd}	R_{ct} (Ω) At the 100^{th}
pristine	4.32	14.99	6.92	21.47	12.04	267.1
3 wt% V_2O_5-coated	6.53	10.69	27.55	23.64	16.31	141.6

Figure Caption

Fig.1. XRD of patterns of (a) $LiNi_{1/3}Co_{1/3}Mn_{1/3}O_2$ and 3 wt% V_2O_5-coated $LiNi_{1/3}Co_{1/3}Mn_{1/3}O_2$; (b) V_2O_5

Fig.2. SEM and TEM of pristine $LiNi_{1/3}Co_{1/3}Mn_{1/3}O_2$ (a), (c) and (e); 3 wt% V_2O_5-coated $LiNi_{1/3}Co_{1/3}Mn_{1/3}O_2$ (b), (d) and (f).

Fig.3. (a) SEM image of 3 wt% V_2O_5-coated $LiNi_{1/3}Co_{1/3}Mn_{1/3}O_2$; (b) EDS spectrum of 3 wt% V_2O_5-coated $LiNi_{1/3}Co_{1/3}Mn_{1/3}O_2$; (c) EDS dot-mapping for V; (d) XPS analysis of V 2p core peaks for 3 wt% V_2O_5-coated $LiNi_{1/3}Co_{1/3}Mn_{1/3}O_2$.

Fig.4. (a) Cycle performance of pristine and different amount of V_2O_5-coated $LiNi_{1/3}Co_{1/3}Mn_{1/3}O_2$ in the voltage range of 2.8-4.5 V at a current of 150 mA/g; (b) Cycle performance of pristine and 3 wt% V_2O_5-coated and $LiNi_{1/3}Co_{1/3}Mn_{1/3}O_2$ at 300 mA/g in the voltage range of 2.8-4.5 V.

Fig.5. (a) Comparison of the initial charge/discharge curves of pristine (black) and 3 wt% V_2O_5-coated $LiNi_{1/3}Co_{1/3}Mn_{1/3}O_2$ (red); (b) Rate capabilities of pristine and 3 wt% V_2O_5-coated $LiNi_{1/3}Co_{1/3}Mn_{1/3}O_2$ in the voltage range of 2.8-4.5 V.

Fig.6. Charge-discharge curves of (a) pristine $LiNi_{1/3}Co_{1/3}Mn_{1/3}O_2$; and (b) 3 wt% V_2O_5-coated $LiNi_{1/3}Co_{1/3}Mn_{1/3}O_2$ at 2 C and at 1^{st} (black), 50^{th} (red) and 100^{th} (green)

Fig.7. Cyclic voltammograms (scan rate of 0.2 mV/s between 2.8 and 4.5 V) of pristine and 3 wt% V_2O_5-coated samples (a) on fresh cells; (b) on cells after 100 cycles of galvanostatic charge-discharge.

Fig.8. EIS Nyquist plots of pristine and 3 wt% V_2O_5-coated materials with cycling, (a) at the 2^{nd} cycle; (b) at the 100^{th} cycle; (c) Voigt-type of equivalent circuit.

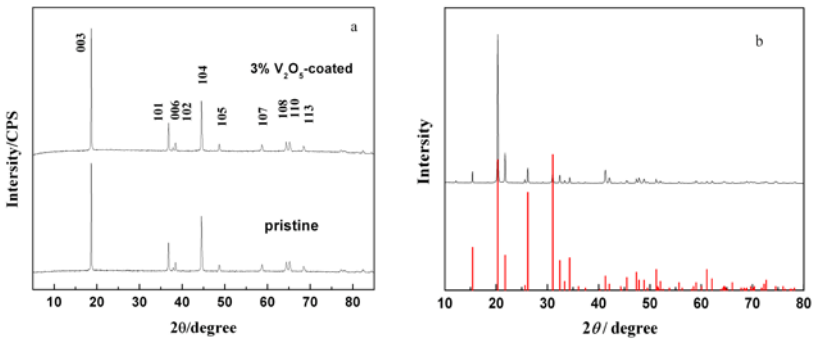
a
003
104
101
006
102
105
107
108
110
113
3% V2O5-coated
pristine
Intersity/CPS
10 20 30 40 50 60 70 80
2θ/degree
b
Intersity
10 20 30 40 50 60 70 80
2θ / degree

Fig. 1.

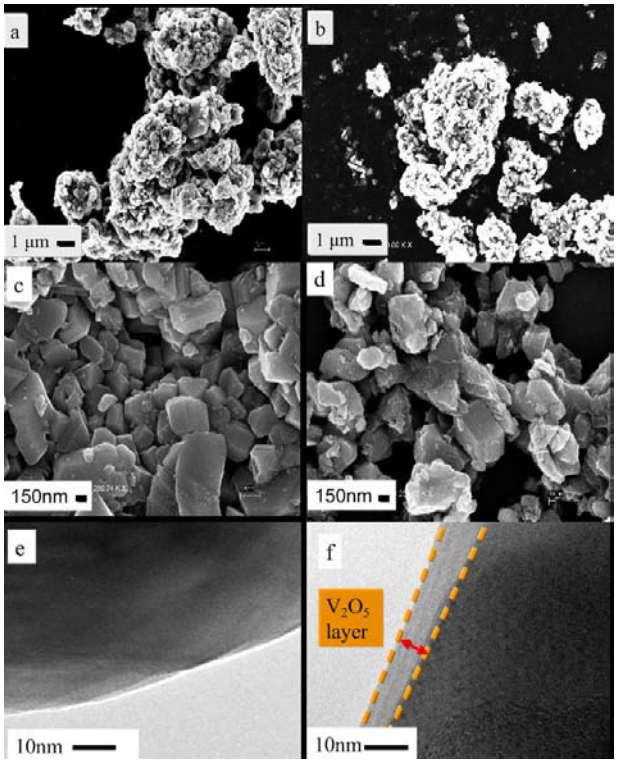
a
1 μm
b
1 μm
c
150nm
d
150nm
e
10nm
f
V2O5
layer
10nm

Fig. 2 .

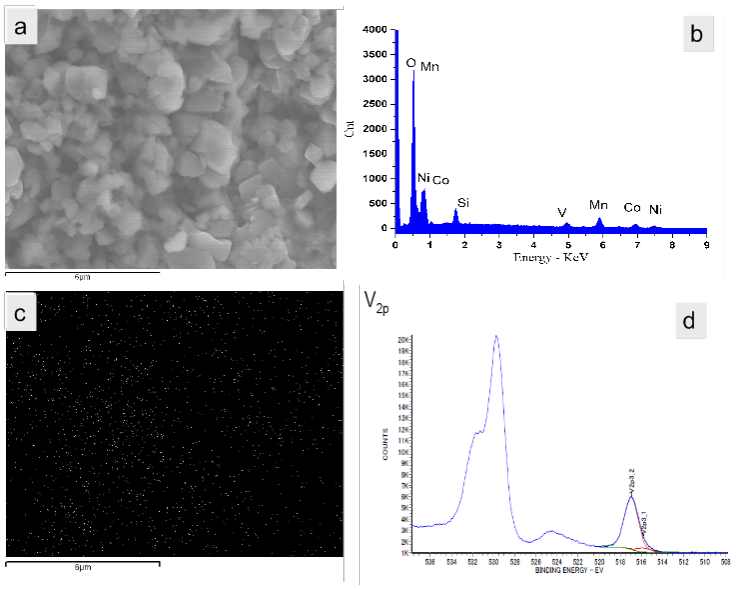

Fig. 3.

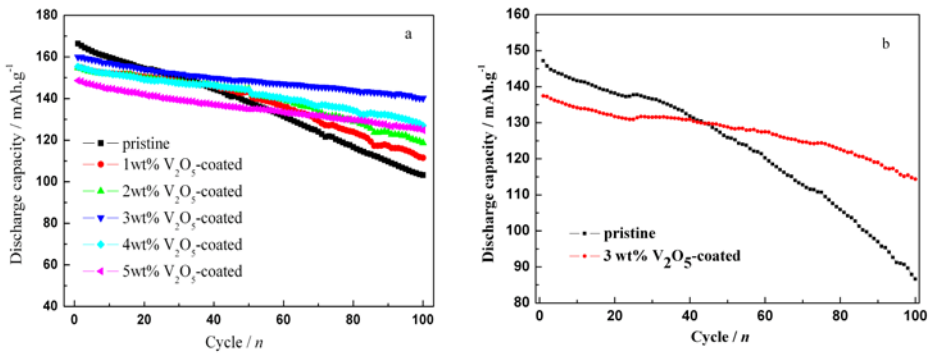

Fig.4.

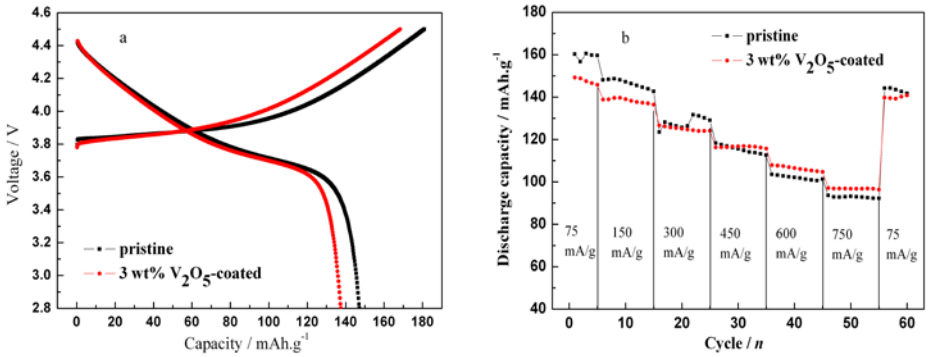

Fig. 5.

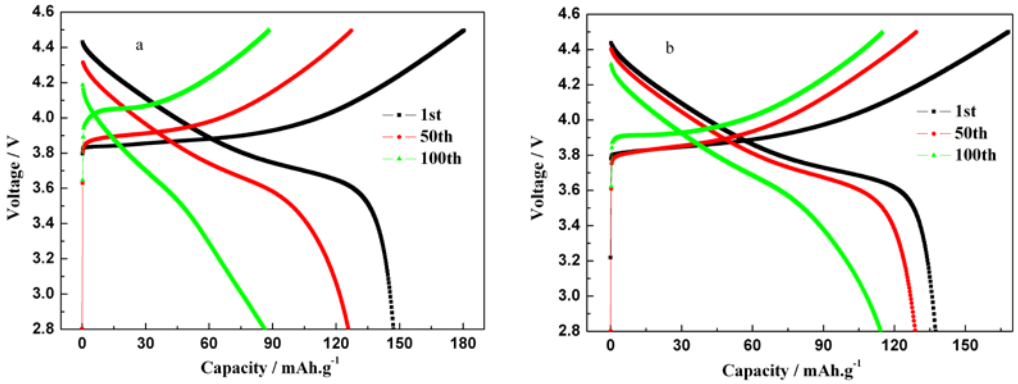

Fig. 6.

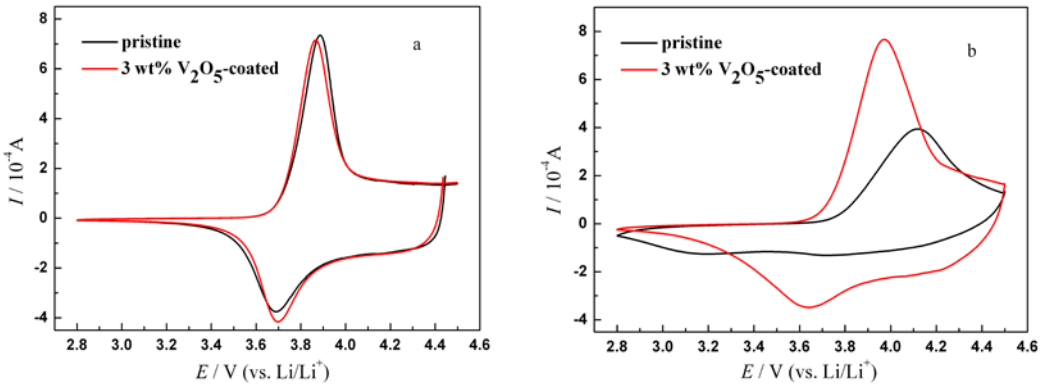

Fig. 7.

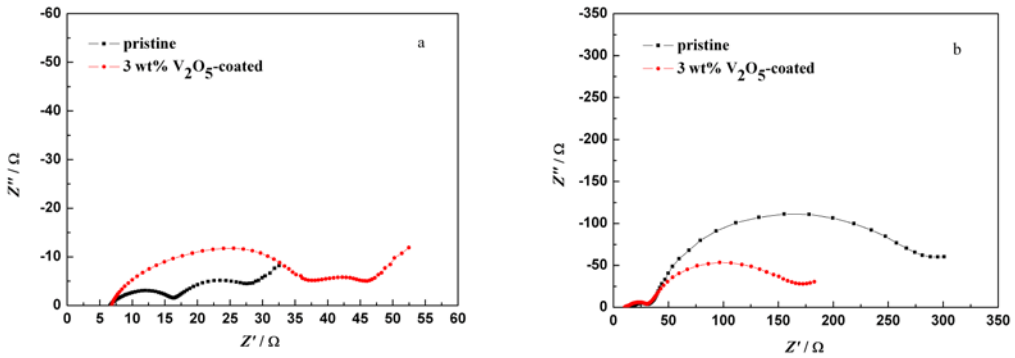

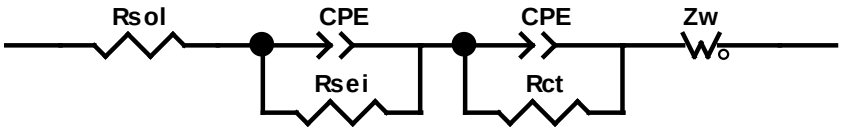

Fig. 8.